Low-Noise Femtosecond SESAM Modelocked Diode-Pumped Cr:ZnS Oscillator

Jonas Heidrich, Ajanta Barh, *Student Member, IEEE*, Sandro L. Camenzind, Benjamin Willenberg, Marco Gaulke, Matthias Golling, Christopher R. Phillips, and Ursula Keller, *Fellow, IEEE*

***Abstract*— Cr-doped ZnS and ZnSe are excellent gain mediums for high power and broadband ultrashort pulse generation in the 2 – 3 μm wavelength range. SESAM modelocked Cr:ZnS oscillators have the advantage of reliable, self-starting passive modelocking. We present a diode-pumped, SESAM modelocked Cr:ZnS oscillator delivering ultrashort pulses of 189 fs at 550 mW average output power with a repetition rate of 435 MHz with low relative intensity noise (RIN) and timing jitter. We measured an integrated RIN of 0.05% within a frequency span of [10 Hz, 5 MHz] dominated by the 1560-nm pump diode, and a very low integrated timing jitter of 10.9 fs [2 kHz, 10 MHz]. This type of laser source benefits not only from very low noise but also from reduced complexity and cost due to direct diode pumping, which is suitable for many applications such as spectroscopy, ranging, and frequency conversion.**

***Index Terms*— Optical frequency comb, diode-pumped ultrafast laser, SESAM modelocking, low-noise source, infrared laser, Cr:ZnS gain medium, transition metal doped II-VI laser.**

I. Introduction

SHORT wavelength infrared (SWIR) modelocked lasers in the 2 – 3 μm wavelength range are of great interest for many applications such as for example atmospheric trace gas sensing, biomedical tissue ablation, or ranging (LIDAR) [1], [2], [3]. Another emerging application area uses ultrashort SWIR pulses for nonlinear frequency conversion into the mid-infrared or soft x-ray regime [4], [5], [6].

Optically pumped chromium (Cr^{2+})-doped II-VI chalcogenide (ZnS and ZnSe, referred to as ZnS(e)) solid-state lasers offer a uniquely broad emission bandwidth in the 2 – 3 μm wavelength range which makes them ideally suited for versatility and ultrashort-pulse generation [7], [8], [9], [10], [11], [12], [13], [14], [15], [16]. These lasers support high-power operation due to favorable thermal properties and the high pump absorption efficiency [15], [17], [18]. Kerr-lens modelocking (KLM) [19] is beneficial for few-cycle pulse generation [11], [16], [20] but requires critical cavity alignment and an external perturbation to start modelocking. In contrast, semiconductor saturable absorber mirror (SESAM) modelocking is favorable for robust, self-starting modelocking [21] with longer transform-limited femtosecond pulses in the soliton modelocking regime [22]. Hence, the SESAM only starts and stabilizes passive modelocking. The final pulse duration is obtained with soliton formation which relaxes the requirement on the recovery time of the SESAM to obtain lower nonsaturable losses and requires no critical cavity alignment close to the stability limit. This also enables higher pulse repetition rates [23] and the ability of compact cavity designs together with low-noise operation [24]. Compared to previous results [8] we recently have demonstrated SESAM modelocked high-power (1 W, 250 MHz, 120 fs, and 0.8 W, 250 MHz, 79 fs) [18] and gigahertz repetition rate (0.8 W, 2 GHz, 155 fs) [25] Cr:ZnS lasers using a high-performance GaSb-based SESAM with strongly reduced nonsaturable losses and a few picosecond recovery time [26], [27]. These lasers have been pumped with a 1.55-μm Er-fiber laser amplifier system.

Direct diode pumping of the gain medium is attractive since this approach drastically reduces the cost and footprint of the pump. A cost reduction for pumping of more than 90% can be achieved with a semiconductor laser diode compared to widely used Er-fiber laser amplifier systems. However, achieving efficient modelocking of a bulk-crystal oscillator is more challenging with diode pumping due to the low beam brightness. Additionally, the noise properties of a diode-pumped SESAM modelocked Cr:ZnS(e) laser have not been investigated to date. Previously a single emitter diode-pumped SESAM modelocked Cr:ZnSe laser has been demonstrated [28], but the laser performance was limited to an average power of 50 mW with 180-fs pulse duration at a pulse repetition rate of 100 MHz. In addition more recently a diode-pumped KLM Cr:ZnSe laser has been demonstrated showing few-cycle pulse generation with lower relative intensity noise (RIN) compared to a fiber-pumped system [16].

Here we demonstrate a diode-pumped Cr:ZnS oscillator using our recently developed SESAMs [18], [27]. We report on a directly diode-pumped SESAM modelocked Cr:ZnS laser achieving stable, self-starting modelocking with 550 mW output power, 189-fs pulses, a pulse repetition rate of 435 MHz at a center wavelength of 2371 nm. The pump laser is a fiber-coupled 1560-nm semiconductor diode laser driven by a low-noise current source to achieve low-noise performance.

Manuscript received 23 August 2022; revised 23 November 2022; accepted 5 January 2023. Date of publication 12 January 2023; date of current version 20 January 2023. This work was supported by the European Research Council (ERC) through the European Union's Horizon 2020 Research and Innovation program under Agreement 787097. *(Corresponding author: Jonas Heidrich.)*

The authors are with the Ultrafast Laser Physics Group, Institute for Quantum Electronics, ETH Zürich, 8093 Zürich, Switzerland (e-mail: hejonas@phys.ethz.ch).

Color versions of one or more figures in this article are available at https://doi.org/10.1109/JQE.2023.3236399.

Digital Object Identifier 10.1109/JQE.2023.3236399

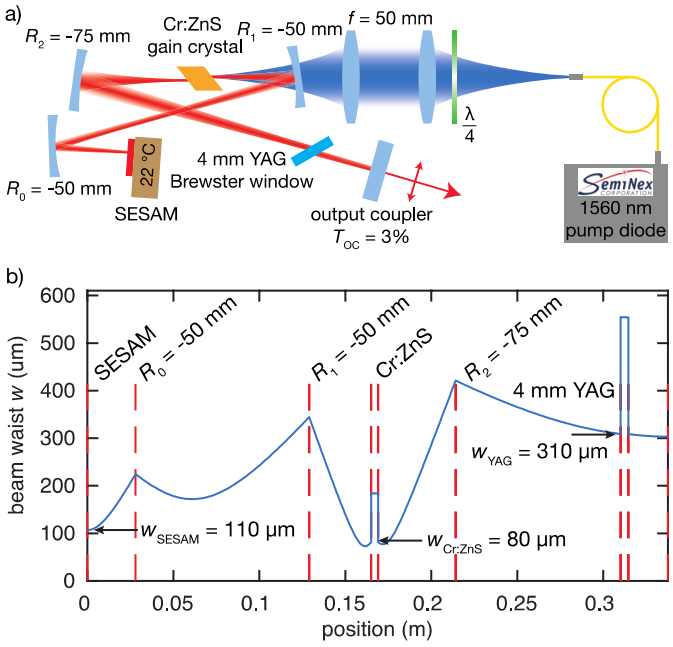

Fig. 1. Laser oscillator design. (a) The X-fold standing-wave cavity consists of the Brewster cut Cr:ZnS gain crystal, three curved mirrors with different radii of curvature R0, R1 and R2, a 4-mm YAG window for dispersion compensation, a SESAM as one end mirror, and a flat output coupler (OC). The cavity is pumped by a fiber-coupled 1560-nm pump diode. (b) Calculated beam waist of the horizontal axis versus cavity position. The red dashed lines highlight positions of intracavity interfaces. A beam radius of 110 µm, 80 µm and 310 µm is achieved at the position of the SESAM, the Cr:ZnS gain medium, and the YAG window, respectively.

The RIN and integrated timing jitter have been characterized. We could show the lowest rms integrated RIN for any Cr:ZnS(e) oscillator of only 0.05% for an integration frequency range of [10 Hz, 5 MHz], and a very low integrated timing jitter of only 10.9 fs integrated over [2 kHz, 10 MHz]. No significant noise is observed for a higher integration limit. We give a detailed description of the cavity design and its modelocking performance. Subsequently, noise characterization methods and results are discussed and guidelines for further noise reduction are given in the conclusion.

II. Laser Design

The diode-pumped Cr:ZnS laser setup employs an X-fold cavity design with a *p*-polarized output beam which is shown in Fig. 1a. The output polarization is defined by Brewster elements in the cavity. All cavity elements are mounted on a transportable optical breadboard and fully boxed using a solid polyvinylchloride housing. The oscillator consists of the gain medium placed between two concave mirrors, the SESAM with a focusing mirror on one side and a 4-mm-long Yttrium-Aluminum-Garnet (YAG) window together with a flat 3% output coupler (OC) on the other side.

Fig. 1b depicts the beam waist throughout the cavity for the horizontal axis using the ABCD-matrix formalism for Gaussian beam propagation. Red dashed lines highlight the positions of intracavity optic interfaces along the beam path.

The Brewster cut, 3.8-mm-long polycrystalline Cr^{2+}:ZnS (chromium doped: zinc sulfide) gain medium (IPG Photonics) has a specified doping concentration of 9.1×10^{18} cm^{-3}. The crystal is contacted with indium foil and mounted on a water-cooled Peltier-controlled copper heat sink stabilized at 16 °C. A three-axis stage combined with a rotation mount allows for optimization of pump threshold and low losses at the crystal facets. All curved intracavity mirrors are ion beam sputtering (IBS) coated (Optoman) for broadband high reflectivity from 2.1 – 3.0 µm and have flat group delay dispersion (GDD). The two concave mirrors with radius of curvature $R_1 = -50$ mm and $R_2 = -75$ mm are placed under an 8° nominal angle of incidence and scale the beam waist to 80 µm in the gain crystal to ensure an optimal overlap with the pump beam. A third curved mirror (radius of curvature $R_0 = -50$mm) is placed under a 12° angle of incidence to compensate for astigmatism originating from intracavity Brewster elements and other curved mirrors and is used to focus the intracavity mode radius to 110 µm on the SESAM. The described cavity properties determine the optical cavity length of 34.5 cm and consequently the repetition rate for fundamental modelocking.

The recently developed, high-quality SESAM is grown with molecular beam epitaxy at the FIRST cleanroom facility, ETH Zurich [26], [27]. It consists of an absorber section with three $In_{0.33}$ $Ga_{0.67}$ Sb quantum wells on top of a 24-pair $AlAs_{0.08}$ $Sb_{0.92}$/GaSb distributed Bragg reflector. The substrate is a (001)-oriented GaSb wafer. The SESAM has a broad stopband of more than 250 nm centered at 2.31 µm. Further, we have characterized the SESAM's nonlinear reflectivity and temporal response under intracavity lasing conditions using 120-fs pulses from an optical parametric oscillator operated near the gain emission peak wavelength at 2.35 µm [26]. From the nonlinear reflectivity measurement [29], we obtain the saturation fluence $F_{sat} = 12\mu J/cm^2$, modulation depth $\Delta R = 1.5\%$, non-saturable losses $R_{ns} = 0.4\%$, and rollover parameter $F_2 = 32mJ/cm^2$. Compared to earlier work in the field [8], the device has substantially lower loss, which enables efficient operation with low output coupling rates. The temporal response is characterized using our pump-probe setup and reveals a very fast recovery within 1 ps due to its strain relaxed quantum well structure (details are given in [27], see SESAM 3). The achieved SESAM parameters are very suitable for fundamental soliton modelocking even for repetition rates in the gigahertz regime [25]. The SESAM is soldered onto a copper mount, which is temperature stabilized using a Peltier element with a passive cooling fin to avoid mechanical vibrations that can arise with water cooling. At a temperature setpoint of 22 °C, stable modelocked laser operation is achieved.

A 4-mm-long YAG window placed at Brewster's angle is used for balancing cavity roundtrip GDD. The plane OC is IBS coated (*University of Neuchâtel*) and the coating has a transmission of 3% over a spectral range from 2.2 – 2.5 µm with a flat, close to zero GDD. The transmission is chosen to provide sufficient intracavity power for modelocked operation.

We pump the cavity with a commercial InP 1560-nm fiber-coupled pump diode delivering up to 5.5 W output power from a 105-µm core diameter multi-mode fiber (*SemiNex Corp.*). This was identified as the most suitable option for a fiber-coupled diode available on the market, even though the gain

crystals absorption peak lies slightly higher at 1680 nm [30]. A low-noise diode driver with a low-noise DC power supply is used as the current source. For optimal stability of the emission wavelength and output power, we have mounted the pump diode on a water-cooled thermoelectrically temperature stabilized heat sink at 23 °C. The beam is collimated using an aspheric lens with a focal length of 50 mm. As the pump exhibits a favorable shift to longer wavelengths for high output powers, we operate it at maximum power and use a large aperture, which is mounted after the collimation lens, for fine-tuning the power on the gain medium. The obtained beam quality was measured with a scanning slit profiler, yielding an M^2 of 17 for a fully opened aperture. The divergence of this low-brightness beam inhibits the use of the pump for positioning the cavity optics. Therefore, we used an external collinear green laser. Although the pump polarization state after the multimode fiber was not linear, by rotating a 1550-nm $\lambda/4$ plate with respect to the fiber output port, we maximize the optical power in the p-polarized plane to 75% in order to reduce Fresnel reflections for the wrong polarization when coupling light into the Brewster-cut gain crystal. Due to space constraints, the $\lambda/4$ plate was placed between the fiber tip and the collimation lens. The collimated pump beam is focused through the input coupler mirror onto the gain crystal with a second 50-mm aspheric lens. The input coupler mirror has a high transmission of 95% at the pump wavelength of 1560 nm. The focal spot size of 75 μm radius is measured with a scanning slit profiler, which is slightly smaller than the cavity mode size of 80 μm. With the given pump configuration, a single pass absorption of 75% in the gain medium is achieved even in non-lasing conditions.

With this laser setup, we achieve fundamental passive modelocking in a normal lab environment at an average output power of 550 mW. The cavity operates in the negative dispersion regime where soliton pulse formation is strongly determined by the balance between negative cavity roundtrip GDD and nonlinear phase shift due to self-phase modulation [22]. The main contribution of -560 fs^2 negative GDD originates from the 4-mm YAG Brewster window whereas most of the nonlinear phase shift happens in the ZnS crystal due to its length combined with the focused cavity mode and a high nonlinear refractive index. In the given soliton modelocking regime, the SESAM serves for self-starting and stabilization of the pulse formation against background radiation. It is operated at an average fluence of 110 μJ/cm^2, close to the rollover point $F_0 \approx 80\mu$J/cm^2 where the maximum reflectivity is reached [18], [25], [31]. We have neither observed any SESAM damage during operation nor during the nonlinear reflectivity characterization where the SESAM is exposed to fluences up to 800 μJ/cm^2 [27].

III. Modelocking Operation

For the pulse characterization during modelocking operation, we use a 13.7-GHz microwave spectrum analyzer (MSA), an optical spectrum analyzer (OSA), and an intensity autocorrelator (AC). As there are no multi-GHz photo detectors (PD) for the 2.4-μm range available, we use a home-built second harmonic generation (SHG) for high-frequency measurements. Here a 5-mm periodically poled lithium niobate crystal is used to convert the laser light to the near-infrared [18]. The converted light is subsequently sampled with a 45-GHz InGaAs photodiode followed by a 25-dB amplifier connected to the MSA for the measurement shown in Fig. 2a. The beam quality was characterized with a bolometer camera and an M^2 measurement using a scanning slit profiler on a linear stage (Fig. 3).

The laser reliably starts modelocked operation at a threshold pump power of 4.6 W on the crystal. The highest output

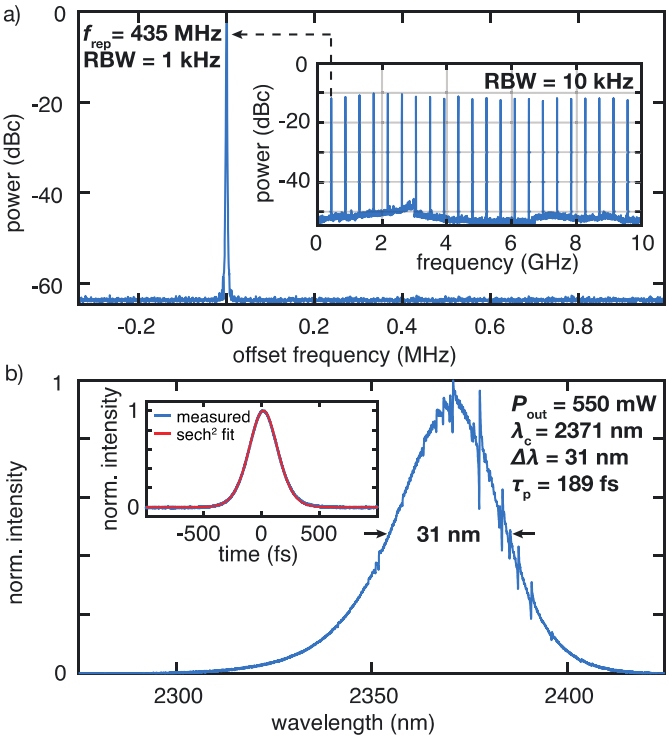

Fig. 2. Modelocking characteristics at 550 mW output power. (a) Microwave spectrum of the frequency-doubled beam recorded with a 45-GHz high-speed PD around the pulse repetition rate of 435 MHz at 1-kHz resolution bandwidth (RBW). Inset: wide span of the microwave spectrum showing equal power distribution of the repetition rate's higher harmonics (RBW = 10 kHz). (b) Normalized optical spectrum sampled with 0.1 nm resolution. Inset: intensity autocorrelation measurement indicating transform-limited 189-fs pulses. The calculated time-bandwidth product is 0.315.

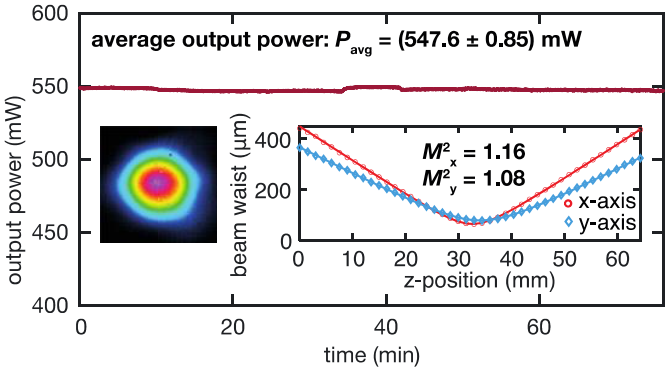

Fig. 3. Laser output power stability and beam characteristics. The average output power of 548 mW is measured at 4.8 W pump power over more than 1 h. This corresponds to rms fluctuations below 0.16%. Inset: bolometer camera image and M2 measurement. The fit for both axes reveals an M2 below 1.16.

power of 550 mW is achieved at a pump power of 4.8 W on the crystal corresponding to an optical-to-optical efficiency of 15.3% considering the output power versus the absorbed pump power. The cavity alignment was performed by not only optimizing for high output power but also maintaining a TEM_{00} mode of the output beam. Higher output powers could only be achieved in higher order mode operation which introduces much more noise.

Another important aspect of cavity alignment is the strong thermal lensing of the gain medium that depends primarily on the pump power. We estimate the thermal lensing parameter as $F_{\mathrm{th}} = 1/f = (P_{\mathrm{abs}}/2\kappa A)(\mathrm{d}n/\mathrm{d}T) \approx 100\ \mathrm{m}^{-1}$, with the absorbed pump power P_{abs}, the thermal conductivity $\kappa = 17\ \mathrm{W/(m \cdot K)}$, the laser beam area A, and the temperature-induced refractive index change $\mathrm{d}n/\mathrm{d}T = 46 \times 10^{-6}\ \mathrm{K}^{-1}$ [32]. Therefore, tuning the cavity such that modelocking operation starts at lower pump powers is feasible, but with the drawback of limited output power scaling.

Fig. 2 shows the modelocking characteristics recorded at 550 mW output power. Using a resolution bandwidth (RBW) of 1 kHz, we obtain a sharp peak with more than 60 dB signal-to-noise ratio at the repetition rate frequency of 435 MHz corresponding to our optical cavity length of 34.5 cm. A wide span MSA spectrum ranging from 0 to 10 GHz exhibits the higher harmonics of the pulse repetition rate with equal power distribution confirming fundamental modelocking (Fig. 2a). The optical spectrum is centered at a wavelength of 2371 nm and has a full width at half maximum (FWHM) bandwidth of 31 nm (Fig. 2b). As the laser is operated in a normal lab environment with 40 – 50% humidity, the spectrum exhibits water absorption features [33]. These features could be removed by nitrogen purging of the boxed cavity [34] but did not influence the laser's modelocking performance. Since purging introduces additional challenges, such as changes to the cavity dispersion and restricted access to the cavity tuning options, we omitted this step and operated in ambient air. The intensity AC measurement reveals transform-limited pulses with a short pulse duration of 189 fs, which corresponds to a pulse peak power of 5.9 kW. Hence, we calculate a time-bandwidth product of 0.315 which is consistent with the expected soliton pulse shaping mechanism [22].

The long-term power stability of the system is shown in Fig. 3. The average output power of 548 mW is recorded for more than one hour with small fluctuations below 0.16% and without any drift. We investigate the beam quality by measuring the beam profile and the M^2 value at the highest power. The measurements, which are shown as insets in Fig. 3, show an M^2 for the x- and y-axis below 1.16 and 1.08, respectively, and a slightly elliptical, single-mode beam shape.

IV. Noise Analysis

Another significant advantage of diode pumping a Cr-doped solid-state laser is its potential for superior noise performance compared to Er-fiber amplifier pumping [13], [25]. Here, we present the one-sided power spectral density (PSD) of the relative intensity noise (RIN) and the timing jitter [35].

The RIN of the modelocked laser output is measured with a high-dynamic-range configuration. A biased InGaAs photodetector with a wavelength cutoff at 2.6 µm and an electronic 3-dB bandwidth of 20 MHz (DET05D2, *Thorlabs*) is installed inside the laser housing and exposed to 0.6 mW of the laser output beam. A focusing lens ensures that the full beam is sampled to prevent additional noise from possible beam-pointing instabilities. For the acquisition of the full RIN spectrum, two subsequent measurements with different amplifiers connected to a signal source analyzer (SSA) are performed [36]. First, we use a low-noise transimpedance amplifier (DLPCA-200, *Femto*) for recording frequency components <200 kHz with optimal sensitivity. Then, higher frequencies (1 kHz – 10 MHz) are measured with a bias-tee (BT45R, *SHF Communication Technologies AG*) splitting AC and DC signal components and a low-noise voltage amplifier (DUPVA-1-70, *Femto*). Both measurement traces are stitched together at about 100 kHz.

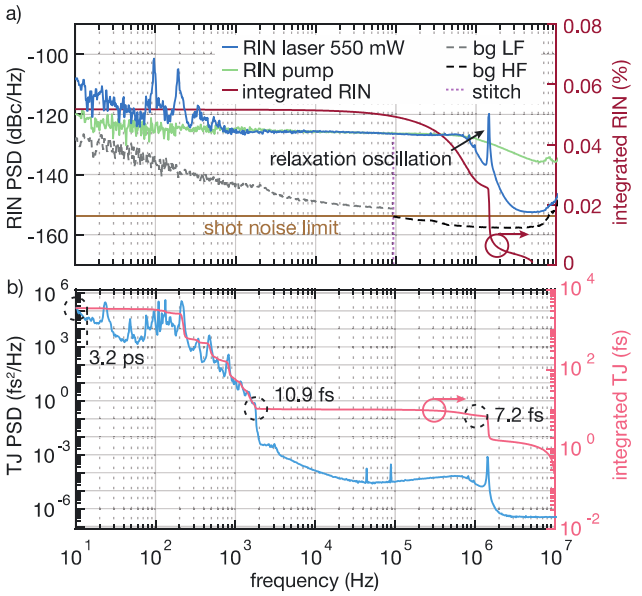

Fig. 4. Power spectral density (PSD) for relative intensity noise (RIN) and timing jitter (TJ). (a) The one-sided PSD for the RIN at maximum output power of 550 mW (blue) and for the pump laser (green) stitched at approximately 100 kHz (see text for more explanation). The background for the low-frequency (bg LF) and high-frequency (bg HF) amplifier is shown in dashed grey and black, respectively. The shot noise limit (brown) is at -153 dBc/Hz. The rms integrated RIN (red) reaches 0.05% [10 Hz, 5 MHz]. (b) One-sided PSD of the timing jitter (light blue) as a function of frequency offset f from the first harmonic (measured at the 35th harmonic and scaled correspondingly) and integrated timing jitter (TJ) (light red). Significant changes in the integrated timing jitter [f, 10 MHz] are marked with dashed circles.

Fig. 4a shows the baseband measurement of the power spectral density (PSD) of the RIN of the laser at full output power and the corresponding RIN spectrum of the pump diode analyzed with the same measurement configuration. We have further measured the electronic noise background of the low-frequency (bg LF) and high-frequency (bg HF) amplifier configuration by blocking the incident laser beam onto the photo detector to ensure a high enough signal-to-noise ratio. The laser noise is dominated by technical noise sources such as mechanical perturbations for frequencies <1 kHz. For higher frequencies >1 kHz, the RIN exhibits a typical plateau behavior [16] which is clearly dominated by the noise from the pump diode. Hence, diode-pumping favors low-noise operation

and reduces the strong noise increase in the multi-kHz regime in comparable Er-fiber pumped Cr:ZnS(e) lasers [13], [25]. At frequencies >1 MHz, the noise is damped because of the limited response time of the Cr:ZnS gain medium. Compared to rare-earth doped crystals, the material responds faster due to its shorter upper-state lifetime and higher cross-section [30]. Slightly above 1 MHz, we observe a spike in the RIN spectrum that contributes significantly to the overall laser noise. We attribute this to be related to the relaxation oscillation of the laser, as it was observed that the intensity and frequency of the peak could be changed while tuning for example the pump power. The shot noise limit at −153 dBc/Hz is reached at a frequency of approximately 5 MHz. When integrating the RIN over [10 Hz, 5 MHz], we obtain an rms noise of only 0.052% which is, to the best of our knowledge, the lowest noise of a Cr:ZnS laser reported so far. Additionally, we have measured the transfer function of the laser [37]. Here, the pump and laser output powers are measured with a lock-in amplifier during a frequency sweep from 10 Hz to 10 MHz with a small (∼1%) sinusoidal current modulation of the diode driver. We again observe a strong feature at the relaxation oscillation frequency of the laser.

To measure the timing jitter of the laser, we detect the pulse train from the SHG frequency conversion setup with a highly linear 22-GHz photodiode (DSC30S, *Discovery Semiconductors inc.*). As with the MSA measurement from Fig. 2a and in earlier work [25], we measure the SHG because of the lack of suitable high-frequency detectors at 2.4 μm. This approach makes the reasonable assumption that the timing jitter is not significantly influenced by the SHG process. The 35^{th} harmonic of the pulse repetition rate is selected with a bandpass filter, amplified, and sampled with the SSA. As the timing jitter PSD around the n^{th} repetition rate harmonic is proportional to n^2, the timing noise is measured at a higher harmonic to improve the measurement sensitivity after normalization to the first harmonic [35]. This also ensures that the noise sidebands are not dominated by the intensity noise. The obtained one-sided timing jitter PSD measured from 10 Hz to 10 MHz is shown in Fig. 4b together with the integrated timing jitter (TJ). The timing jitter PSD follows the qualitative behavior of the laser RIN, which is expected as RIN can couple to timing jitter [38], [39]. The influence of the relaxation oscillation peak above 1 MHz raises the integrated timing jitter to a value of 7.2 fs. Nevertheless, when integrating from 2 kHz – 10 MHz a very low timing jitter of 10.9 fs is obtained. When including the influence of lower frequencies down to 10 Hz in the timing jitter calculation, the jitter accumulates to 3.2 ps. This increase can be explained by mechanical noise sources. The stability at low frequencies would benefit significantly from a fully integrated prototype setup and active stabilization [38], which goes beyond the scope of this paper. Overall, the low timing jitter at electronic noise frequencies indicates the ability of diode-pumping for highly stable low-noise laser systems.

V. Conclusion

In summary, we have demonstrated a directly diode-pumped SESAM modelocked Cr:ZnS laser delivering low-noise modelocked pulses in the molecular fingerprint region above 2 μm. This new type of laser only needs a low-cost multimode near-infrared (1560 nm) pump diode together with a low-noise power supply which substantially reduces the system footprint and complexity. Self-starting passive modelocking is achieved by using an in-house grown high-performance GaSb SESAM. Transform-limited 189-fs pulses at a repetition rate of 435 MHz are obtained at a high average output power of 550 mW, corresponding to a peak power of 5.9 kW. Further power scaling efforts would benefit from high-brightness and high-power pump diodes ideally at the peak absorption wavelength of 1680 nm. The laser delivers a long-term stable output power together with a good beam quality ($M^2 < 1.16$ for both axes).

Noise analysis of the free-running Cr-doped ZnS laser at standard lab conditions reveals a record-low integrated rms RIN of only 0.05% [10 Hz, 5 MHz] and a low integrated timing jitter of 10.9 fs [2 kHz, 10 MHz]. Wavelength stabilized pump diodes could improve the noise performance even further. Finally, the presented result demonstrates the capabilities of this type of laser: reliable self-starting SESAM modelocking, a cost-effective and low complexity pumping scheme, and highly stable low-noise performance. This paves the way towards compact SWIR laser-based precision frequency metrology, spectroscopy, and nonlinear frequency conversion.

Acknowledgment

The authors thank Dr. V. Wittwer of University of Neuchâtel for providing the IBS coating on the output coupler. They acknowledge the support of FIRST clean room facility of ETH Zürich.

References

[1] K. Scholle, S. Lamrini, P. Koopmann, and P. Fuhrberg, "2 μm laser sources and their possible applications," in *Frontiers in Guided Wave Optics and Optoelectronics*. Rijeka, Croatia: InTech, 2010.

[2] N. M. Fried, "Recent advances in infrared laser lithotripsy [invited]," *Biomed. Opt. Exp.*, vol. 9, no. 9, p. 4552, Sep. 2018, doi: 10.1364/boe.9.004552.

[3] D. Grassani et al., "Mid infrared gas spectroscopy using efficient fiber laser driven photonic chip-based supercontinuum," *Nature Commun.*, vol. 10, no. 1, pp. 1–8, Apr. 2019, doi: 10.1038/s41467-019-09590-3.

[4] D. Sanchez et al., "7 μm, ultrafast, sub-millijoule-level mid-infrared optical parametric chirped pulse amplifier pumped at 2 μm," *Optica*, vol. 3, no. 2, p. 147, Feb. 2016, doi: 10.1364/optica.3.000147.

[5] V. E. Leshchenko et al., "High-power few-cycle Cr:ZnSe mid-infrared source for attosecond soft X-ray physics," *Optica*, vol. 7, no. 8, pp. 981–988, Aug. 2020, doi: 10.1364/OPTICA.393377.

[6] P. Steinleitner et al., "Single-cycle infrared waveform control," *Nature Photon.*, vol. 16, no. 7, pp. 512–518, May 2022, doi: 10.1038/s41566-022-01001-2.

[7] C. R. Pollock et al., "Mode locked and Q-switched Cr:ZnSe laser using a semiconductor saturable absorbing mirror (SESAM)," in *Proc. Advanced Solid-State Photonics*, 2005, pp. 15–17, doi: 10.1364/assp.2005.tua6.

[8] E. Sorokin, N. Tolstik, K. I. Schaffers, and I. T. Sorokina, "Femtosecond SESAM-modelocked Cr:ZnS laser," *Opt. Exp.*, vol. 20, no. 27, p. 28947, Dec. 2012, doi: 10.1364/OE.20.028947.

[9] M. N. Cizmeciyan, J. W. Kim, S. Bae, B. H. Hong, F. Rotermund, and A. Sennaroglu, "Graphene mode-locked femtosecond Cr:ZnSe laser at 2500 nm," *Opt. Lett.*, vol. 38, no. 3, p. 341, Feb. 2013, doi: 10.1364/ol.38.000341.

[10] I. T. Sorokina and E. Sorokin, "Femtosecond Cr^{2+}-based lasers," *IEEE J. Sel. Topics Quantum Electron.*, vol. 21, no. 1, pp. 273–291, Jan. 2015, doi: 10.1109/JSTQE.2014.2341589.

[11] S. Vasilyev, I. Moskalev, M. Mirov, S. Mirov, and V. Gapontsev, "Three optical cycle mid-IR Kerr-lens mode-locked polycrystalline Cr^{2+}:ZnS laser," *Opt. Lett.*, vol. 40, no. 21, p. 5054, 2015, doi: 10.1364/ol.40.005054.

[12] S. Vasilyev et al., "Ultrafast middle-IR lasers and amplifiers based on polycrystalline Cr:ZnS and Cr:ZnSe," *Opt. Mater. Exp.*, vol. 7, no. 7, pp. 2636–2650, Jul. 2017, doi: 10.1364/OME.7.002636.

[13] Y. Wang, T. T. Fernandez, N. Coluccelli, A. Gambetta, P. Laporta, and G. Galzerano, "47-fs Kerr-lens mode-locked Cr:ZnSe laser with high spectral purity," *Opt. Exp.*, vol. 25, no. 21, p. 25193, Oct. 2017, doi: 10.1364/oe.25.025193.

[14] S. B. Mirov et al., "Frontiers of mid-IR lasers based on transition metal doped chalcogenides," *IEEE J. Sel. Topics Quantum Electron.*, vol. 24, no. 5, pp. 1–29, Sep. 2018, doi: 10.1109/JSTQE.2018.2808284.

[15] S. Vasilyev et al., "Super-octave longwave mid-infrared coherent transients produced by optical rectification of few-cycle 25-μm pulses," *Optica*, vol. 6, no. 1, p. 111, Jan. 2019, doi: 10.1364/OPTICA.6.000111.

[16] N. Nagl, S. Gröbmeyer, V. Pervak, F. Krausz, O. Pronin, and K. F. Mak, "Directly diode-pumped, Kerr-lens mode-locked, few-cycle Cr:ZnSe oscillator," *Opt. Exp.*, vol. 27, no. 17, p. 24445, Aug. 2019, doi: 10.1364/oe.27.024445.

[17] E. Sorokin, N. Tolstik, and I. T. Sorokina, "1 Watt femtosecond mid-IR Cr: ZnS laser," *Proc. SPIE*, vol. 8599, no. 6, Mar. 2013, Art. no. 859916, doi: 10.1117/12.2003877.

[18] A. Barh et al., "Watt-level and sub-100-fs self-starting mode-locked 24-μm Cr: ZnS oscillator enabled by GaSb-SESAMs," *Opt. Exp.*, vol. 29, no. 4, p. 5934, Feb. 2021, doi: 10.1364/oe.416894.

[19] D. E. Spence, P. N. Kean, and W. Sibbett, "60-fsec pulse generation from a self-mode-locked Ti: Sapphire laser," *Optics Letters*, vol. 16, no. 1, pp. 42–44, 1991.

[20] S. Vasilyev et al., "Middle-IR frequency comb based on Cr:ZnS laser," *Opt. Exp.*, vol. 27, no. 24, p. 35079, 2019, doi: 10.1364/oe.27.035079.

[21] U. Keller et al., "Semiconductor saturable absorber mirrors (SESAM's) for femtosecond to nanosecond pulse generation in solid-state lasers," *IEEE J. Sel. Top. Quantum Electron.*, vol. 2, no. 3, pp. 435–453, Sep. 1996, doi: 10.1109/2944.571743.

[22] F. X. Kartner, I. D. Jung, and U. Keller, "Soliton mode-locking with saturable absorbers," *IEEE J. Sel. Topics Quantum Electron.*, vol. 2, no. 3, pp. 540–556, Sep. 1996, doi: 10.1109/2944.571754.

[23] A. S. Mayer, C. R. Phillips, and U. Keller, "Watt-level 10-gigahertz solid-state laser enabled by self-defocusing nonlinearities in an aperiodically poled crystal," *Nature Commun.*, vol. 8, no. 1, pp. 1–8, Nov. 2017, doi: 10.1038/s41467-017-01999-y.

[24] S. Schilt et al., "Noise properties of an optical frequency comb from a SESAM-mode-locked 1.5-μm solid-state laser stabilized to the 10–13 level," *Appl. Phys. B, Lasers Optics*, vol. 109, no. 3, pp. 391–402, Nov. 2012, doi: 10.1007/s00340-012-5072-z.

[25] A. Barh et al., "High-power low-noise 2-GHz femtosecond laser oscillator at 2.4 μm," *Opt. Exp.*, vol. 30, no. 4, p. 5019, Feb. 2022, doi: 10.1364/oe.446986.

[26] J. Heidrich, M. Gaulke, B. O. Alaydin, M. Golling, A. Barh, and U. Keller, "Full optical SESAM characterization methods in the 1.9 to 3-μm wavelength regime," *Opt. Exp.*, vol. 29, no. 5, p. 6647, Mar. 2021, doi: 10.1364/oe.418336.

[27] B. Ö. Alaydin, M. Gaulke, J. Heidrich, M. Golling, A. Barh, and U. Keller, "Bandgap engineering, monolithic growth, and operation parameters of GaSb-based SESAMs in the 2–2.4 μm range," *Opt. Mater. Exp.*, vol. 12, no. 6, p. 2382, Jun. 2022, doi: 10.1364/ome.459232.

[28] E. U. Slobodtchikov and P. F. Moulton, "Progress in ultrafast Cr:ZnSe lasers," in *Proc. Adv. Solid-State Photon. (ASSP)*, 2012, pp. 9–10, doi: 10.1364/assp.2012.aw5a.4.

[29] M. Haiml, R. Grange, and U. Keller, "Optical characterization of semiconductor saturable absorbers," *Appl. Phys. B*, vol. 79, no. 3, pp. 331–339, Aug. 2004, doi: 10.1007/s00340-004-1535-1.

[30] I. T. Sorokina, "Cr2+-doped II–VI materials for lasers and nonlinear optics," *Opt. Mater.*, vol. 26, no. 4, pp. 395–412, Sep. 2004, doi: 10.1016/j.optmat.2003.12.025.

[31] C. J. Saraceno et al., "SESAMs for high-power oscillators: Design guidelines and damage thresholds," *IEEE J. Sel. Topics Quantum Electron.*, vol. 18, no. 1, pp. 29–41, Jan. 2012, doi: 10.1109/JSTQE.2010.2092753.

[32] K. L. Schepler, R. D. Peterson, P. A. Berry, and J. B. McKay, "Thermal effects in Cr^{2+}: ZnSe thin disk lasers," *IEEE J. Sel. Topics Quantum Electron.*, vol. 11, no. 3, pp. 713–720, May 2005, doi: 10.1109/JSTQE.2005.850570.

[33] V. L. Kalashnikov and E. Sorokin, "Soliton absorption spectroscopy," *Phys. Rev. A, Gen. Phys.*, vol. 81, no. 3, Mar. 2010, Art. no. 033840, doi: 10.1103/physreva.81.033840.

[34] N. Tolstik, E. Sorokin, and I. T. Sorokina, "Graphene mode-locked Cr:ZnS laser with 41 fs pulse duration," *Opt. Exp.*, vol. 22, no. 5, p. 5564, Mar. 2014, doi: 10.1364/oe.22.005564.

[35] U. Keller, *Ultrafast Lasers*. Cham, Switzerland: Springer, 2021.

[36] J. Pupeikis et al., "Spatially multiplexed single-cavity dual-comb laser," *Optica*, vol. 9, no. 7, p. 713, Jul. 2022, doi: 10.1364/optica.457787.

[37] A. Schlatter, S. C. Zeller, R. Grange, R. Paschotta, and U. Keller, "Pulse-energy dynamics of passively mode-locked solid-state lasers above the Q-switching threshold," *J. Opt. Soc. Amer. B, Opt. Phys.*, vol. 21, no. 8, p. 1469, Aug. 2004, doi: 10.1364/josab.21.001469.

[38] R. Paschotta, H. R. Telle, and U. Keller, "Noise of solid-state lasers," in *Solid-State Lasers and Applications*, A. Sennaroglu, Ed. Boca Raton, FL, USA: CRC Press, 2007, pp. 473–510.

[39] M. Endo, T. D. Shoji, and T. R. Schibli, "Ultralow noise optical frequency combs," *IEEE J. Sel. Topics Quantum Electron.*, vol. 24, no. 5, pp. 1–13, Sep. 2018, doi: 10.1109/JSTQE.2018.2818461.

Jonas Heidrich born in Karlsruhe, Germany, in 1992. He received the B.Sc. and M.Sc. degrees in physics from the Karlsruhe Institute of Technology, Karlsruhe, in 2015 and 2018, respectively. He graduated with research projects on x-ray interferometry and thermoelectric effects of superconducting nanostructures. He is currently pursuing the Ph.D. degree with the Ultrafast Lasers Physics Group, ETH Zurich, Zurich, Switzerland. His research work is focused on the development of infrared GaSb semiconductor saturable absorbers for modelocked semiconductor and solid-state frequency combs. His interests include device design and fabrication, laser characterization, and ultrafast measurement techniques.

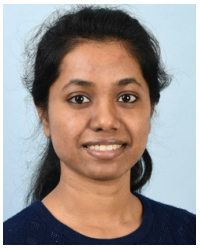

Ajanta Barh (Student Member, IEEE) received the Ph.D. degree in physics from the Indian Institute of Technology Delhi, New Delhi, India, in 2015. In 2016, she joined at the Optical Sensor Technology Group, DTU Fotonik, Technical University of Denmark as a Post-Doctoral, where she developed frequency upconversion based rapid broadband optical detection systems for mid-infrared sensing and imaging. In 2019, she joined at the Ultrafast Laser Physics Group, Department of Physics, ETH Zurich, as a Senior Post-Doctoral/Subgroup Leader, where currently she is working on ultrafast solid state and semiconductor laser systems operating in the shortwave-infrared, towards application in frequency metrology and sensing. She has authored/coauthored more than 60 peer-reviewed journal and conference publications. Her current research interests include mid-infrared photonics, ultrafast lasers and application, nonlinear optics, upconversion detection, and specialty optical fibers. She is a Senior Member of OPTICA (formerly OSA). She is also a Program Committee Member of international conference IEEE WRAP in 2017 and 2019, and UFO XIII from 2022 to 2023, and a Review Committee Member of OPTICA Women Scholars Program in 2022 and OPTICA Siegman International School on Lasers from 2019 to 2022. She was the Chair of OPTICA Nonlinear Optics Technical Group from 2018 to 2020 and the Vice-Chair from 2021 to 2023.

Sandro L. Camenzind was born in Stans, Switzerland, in 1995. He received the M.Sc. degree in physics from ETH Zurich, Switzerland, in 2020, where he is currently pursuing the Ph.D. degree in physics. His research at the Ultrafast Laser Physics Group of Prof. Ursula Keller focuses on developing and characterizing single-and dual optical frequency comb sources.

Benjamin Willenberg was born in Goch, Germany, in 1988. He received the B.Sc. degree in mathematics and the M.Sc. degree in physics from the University of Göttingen in 2013 and 2014, respectively, and the Ph.D. degree in physics from ETH Zurich for work in the field of strong-field-ionization and attosecond science, and highly efficient high power frequency conversion from the NIR into the DUV, in 2019. Since 2019, he has been a Post-Doctoral Researcher with the Ultrafast Laser Physics Group of Prof. Keller at ETH Zurich. His research interests include development of low-noise single-cavity dual-comb oscillators and their applications in science and industry.

Marco Gaulke was born in Mannheim, Germany, in 1993. He received the bachelor's and master's degrees in physics from the Karlsruhe Institute of Technology, in 2015 and 2018, respectively. After modeling physiosorption processes in his bachelor's thesis, he investigated carbon nanotube electroluminescence at low temperature during his master's thesis. During his studies he was a Scholarship Holder at the German Academic Scholarship Foundation. He is pursuing the Ph.D. degree with the Ultrafast Laser Physics Group, ETH Zurich. His research interests include transferring the semiconductor-based VECSEL and MIXSEL technology further into the infrared.

Matthias Golling was born in Sulz/Neckar, Germany, in 1971. He received the Dipl.-Ing. and Dr.-Ing. degrees in electrical engineering from the University of Ulm, Ulm, Germany, in 1997 and 2004, respectively. In 1996, he was with NTT Optoelectronic Labs, Ibaraki, Japan, investigating erbium-doped waveguides. Since 2002 he has been with the Institute of Quantum Electronics, ETH Zurich, Switzerland. During the first year at ETH his research interests were focused on the crystal growth of high-speed electronic and optoelectronic devices with molecular beam epitaxy. The growth of both laser structures and record saturable absorber structures (SESAMs) on GaAs dominated the following years. Since 2019 his research broadened to the growth of GaSb-based materials to transfer the successful laser technology to the 2-micrometer wavelength range and above.

Christopher R. Phillips received the M.S. and Ph.D. degrees in electrical engineering from Stanford University in 2009 and 2012, respectively. He worked at Stanford on nonlinear optical devices for pulsed and continuous wave photonic applications. Following his Ph.D. degree, he moved to ETH Zurich, Ultrafast Laser Physics Group via a Marie Curie fellowship on optical parametric chirped pulse amplification. After the fellowship, he stayed at ETH while broadening. He is the Senior Project Leader for the Solid-State Frequency Combs Subgroup. He has coauthored about 60 journal publications and 120 conference papers. His current research interests include modelocked lasers and parametric oscillators with low-noise, high repetition rate, and high power applications of dual optical frequency combs, and numerical modeling of nonlinear-optical systems. He is a Senior Member of Optica.

Ursula Keller (Fellow, IEEE) received the Diploma degree in physics from ETH, in 1984, and the Ph.D. degree from Stanford University, in 1989. She was a Director at the Swiss Multi-Institute NCCR MUST Program in ultrafast science from 2010 to 2022. She was a Visiting Miller Professor at UC Berkeley, in 2006 and a Visiting Professor at the Lund Institute of Technologies, in 2001. She has been a Tenured Professor of physics with ETH Zurich since 1993. She supervised and graduated 91 Ph.D. students (list), published more than 490 journal publications and according to Google Scholar an h-index of 116 with more than 50'000 citations. Her research interests include exploring and pushing the frontiers in ultrafast science and technology. She was a Member of Technical Staff (MTS) at AT&T Bell Laboratories from 1989 to 1993. She was also a member of the research council at the Swiss National Science Foundation from 2014 to 2018. She is the Founding President at the ETH Women Professors Forum. She is a member of the USA. National Academy of Sciences, Royal Swedish Academy of Sciences, and German Academy Leopoldina and Swiss Academy of Technical Sciences. She has been a Co-founder and a board member for Time-Bandwidth Products (acquired by JDSU in 2014) and for a Venture Capital Funded Telecom Company GigaTera (acquired by Time-Bandwidth in 2003). She received the awards include the OSA Frederic Ives Medal/Jarus W. Quinn Prize in 2020-OSA's (resp. OPTICA's) highest award for overall distinction in optics, the SPIE Gold Medal in 2020-SPIE's highest honor, the IEEE Edison Medal in 2019, the IEEE Photonics Award in 2018, the European Inventor Award for lifetime achievement 2018, and the two ERC advanced Grants in 2012 and 2018.